INTERNATIONAL ATOMIC ENERGY AGENCY
UNITED NATIONS EDUCATIONAL, SCIENTIFIC AND CULTURAL ORGANIZATION
INTERNATIONAL CENTRE FOR THEORETICAL PHYSICS
I.C.T.P., P.O. BOX 586, 34100 TRIESTE, ITALY, CABLE: CENTRATOM TRIESTE

H4.SMR/645-5

SCHOOL ON PHYSICAL METHODS FOR THE STUDY OF THE UPPER AND LOWER ATMOSPHERE SYSTEM

26 October - 6 November 1992
Miramare - Trieste, Italy

Atmospheric Signals at High Latitudes in a Coupled Ocean-Atmosphere General Circulation Model

Sultan Hameed
State University of New York
Stony Brook, NY
USA

MAIN BUILDING STRADA COSTIERA, 11 TEL. 22401 TELEFAX 224163 TELEX 460392 ADRIATICO GUEST HOUSE VIA GRIGNANO, 9 TEL. 224241 TELEFAX 224531 TELEX 460449
MICROPROCESSOR LAB. VIA BEIRUT, 31 TEL. 224471 TELEFAX 224600 TELEX 460392 GALILEO GUEST HOUSE VIA BEIRUT, 7 TEL. 22401 TELEFAX 224559 TELEX 460392

GEOPHYSICAL RESEARCH LETTERS, VOL. 17, NO. 7, PAGES 945-948, JUNE 1990

ATMOSPHERIC SIGNALS AT HIGH LATITUDES IN A COUPLED OCEAN-ATMOSPHERE GENERAL CIRCULATION MODEL

Robert G. Currie and Sultan Hameed

State University of New York at Stony Brook

Abstract. We report evidence for a ca. 40 month signal in air pressure simulated in a general circulation model, together with two further natural signals previously found, the ca. 26 month quasi-biennial oscillation (QBO) and the ca. 14 month atmospheric Chandler tide. These 3 natural signals interact with the annual cycle and its harmonics to create a rich spectrum of summation and difference tones. Theoretically we expect 33 tones to be produced and evidence for 29 of these is found. The three classes of signals combined to contribute 51% of total variance, and range in period from 2 to 68 months. These results indicate that the spectrum of atmospheric variations on these time scales is discrete, unlike that of a chaotic system.

Introduction

Study of air pressure variations simulated in two General Circulation Models led to reports of several atmospheric oscillations [Currie and Hameed, 1988; Hameed and Currie, 1989]. Two were identified as the quasi-biennial oscillation (or QBO) with period ca. 26 months, and the atmospheric Chandler wobble of period ca. 14.7 months. We also found spectral peaks near 10 and 6.7 months which were explained as the interaction of the Chandler signal with the annual term and its 6 month harmonic; it was further pointed out that another term near 66 months should also eventually be detected.

Such terms (the 66, 10, and 6.7 month terms) are called "combination tones" in nonlinear mechanics, and they are generated when the damping term in the equations of motion varies quadratically [Stoker, 1950, p. 113]. A familiar example, originally invoked by Helmholtz, is the human ear where tones of frequencies f_2-f_1 (the "difference tone") and f_2+f_1 (the "summation tone") are often heard when two notes of frequencies f_1 and f_2 are sounded.

The Oregon State University General Circulation Model (OSU GCM) calculates atmospheric pressure and other climatic variables around the globe. In this note we present the spectrum of simulated atmospheric pressure for high northern latitudes; this region is of particular interest because it is known to be characterized by large climatic variability. The results presented here show that half of this variability is contained in band-limited signals of known physical origin.

In addition to the signals mentioned above (with periods of ca. 26, and 14.7 months) the high latitude region shows another in the subannual time scale with period ca. 40 months which we propose represents one signature of ENSO and denote as the quasi-triennial oscillation, QTO, [a time domain analysis of the southern oscillation in the OSU GCM is presented by Sperber et al. (1987), Hameed et al. (1989), and Sperber (1989)]. For monthly sampled data, the QTO, the QBO, and the Chandler signal would interact with the annual cycle and its harmonics at 6, 4, 3, 2.4, and 2 months to theoretically produce 33 difference and summation tones. We report evidence that the GCM has simulated 29 of these 33 tones at 216 locations between 74^o and 82^o latitude north.

Analysis

We examine the simulated surface atmospheric pressures from the Oregon State University coupled ocean-atmosphere GCM at high latitudes. The horizontal resolution is 4^o in latitude and 5^o in longitude. The model has a 2 layer atmosphere and 6 layers in the ocean. The model will be referred to as OSU6 GCM in the following. The atmosphere and the ocean interact according to the conventional bulk formulae, with sea-surface temperature internally predicted. The model calculation included diurnal and seasonal variations of solar radiation. An integration of the model equations was carried out for 20 simulated years. The formulation of the model and the global distributions characterizing the mean simulated climate have been presented by Gates et al. (1985).

We have analyzed the time series of 240 monthly values of surface atmospheric pressure at each of the 3312 grid points. After subtracting the mean value of surface air pressure from each series, the Fourier transform was calculated and results for 216 spectra from latitudes 74^o to 82^o north are displayed in Figure 1a. Confining attention to periods 6 months or longer, we observe the annual cycle and its 1st harmonic at 6 months as well as the 6 terms discussed previously: the 26.7 month QBO, the 14.5 month Chandler wobble, the summation tone at 6.7 months due to the Chandler and annual term, and the difference tones at 68.7 and 10.3 months due to the Chandler term interacting with the annual and 6 month harmonic, respectively. Also shown is a peak at 40 months. At higher frequencies arrows point to the higher harmonics of the annual cycle at 3.96, 3.04, 2.4, and 2 months.

Omitting the annual and its harmonics, a background spectrum was computed for each of the 216 spectra in 6 swaths, each swath extending over 20 frequency estimates. Six swaths were chosen to ameliorate the effect of the slightly 'pink' nature of the continuum, and this background is given by the dashed horizontal lines seen in Figure 1a. For each spectrum the ratio A_i of the spectral estimate to the background spectrum was determined for frequencies f_i = i/240, i = 1 to

Paper number 90GL01018
0094-8276/90/90GL-01018$03.00

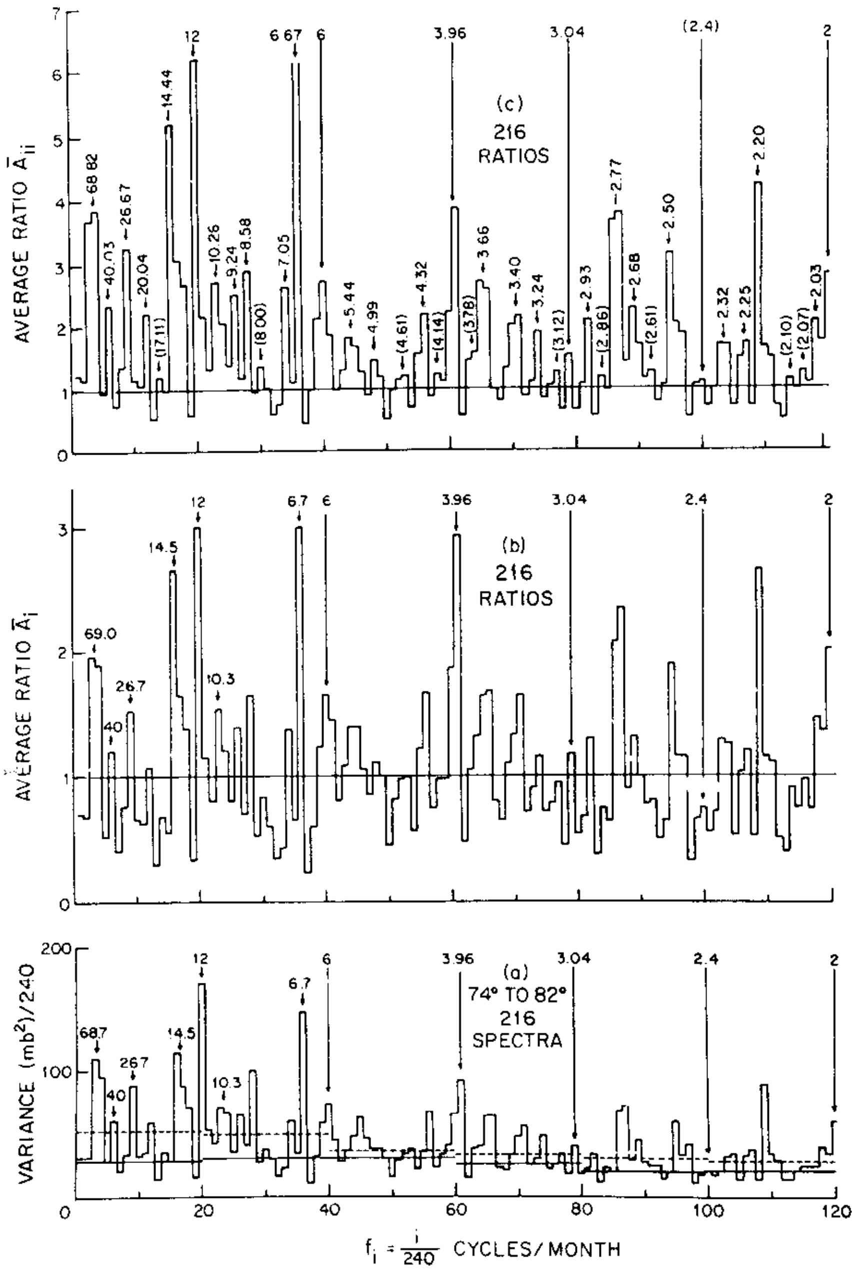

Fig. 1. Average Fourier spectra for the 216 grid locations between 74°N and 82°N. Figure 1(a), bottom panel, gives the distribution of variance with frequency. Periods in months are shown with arrows pointing to some peaks discussed in the text. Figure 1(b) gives the average value of the ratios of the spectral estimates to the background spectrum. The peaks found to be significantly different from the background are subtracted from it to obtain a new set of spectral ratios shown in Figure 1(c), top panel.

120. For each frequency f_i the mean value $\bar{A}_i$ and the standard deviation of the ratios A_i were computed. The mean spectral ratios $\bar{A}_i$ are shown in Figure 1b. There are 29 peaks above unity, indicating that these are signals. The t-statistic may be used to test the significance of the result that $\bar{A}_i > 1$ for these frequencies. Although the ratios in Figure 1b represents the average of 216 spectra, the number of applicable degrees of freedom is likely to be smaller because of correlation in atmospheric pressure over neighboring regions. The t-statistics for the 29 frequencies with $\bar{A}_i > 1$ had values between 1.6 and 14.6 with the mean value 5.0. In the table for t-statistic we note that the mean value corresponds to 8 degrees of freedom for 99.9% significance and 3.5 degrees of freedom for 99% significance. Although there is no straightforward procedure for estimating the effective number of degrees of freedom we see that the number required to estab-

lish statistical confidence that the ratios $\bar{A}_i$ exceed unity is much less than 216.

It is now seen that the estimated background noise included a large number of signals and is, therefore, too high. We obtained a new background spectrum by subtracting the variance of all peaks in Figure 1b with $\bar{A}_i > 1$. The new background is shown by the solid horizontal lines in Figure 1a, and the new mean ratios $\bar{A}_{ii}$ are plotted in Figure 1c. Note that the ordinate scale has increased by a factor of 2. The arrows and associated numbers represent the mean period of every peak above unity. A further 11 signals have emerged and their periods are bracketed (the 4th harmonic of the annual term is now recognized as a signal). The t-statistics of the 40 peaks in Figure 1c are between 2.1 and 17.7 with a mean value of 7.1, so the statistical significance of the 40 peaks is high.

In a longer paper we present evidence that the OSU6 GCM displays the signals shown in Figure 1 throughout the globe and that these signals also characterize atmospheric observations [Hameed et al., 1990]. We have also analyzed the frequency characteristics of an independent realization of climate in the OSU2 GCM (version of the OSU GCM in which the ocean is represented by two layers i.e., the mixed layer and the thermocline) which corroborate those found for the OSU6 model. Previously Currie and Hameed (1988) reported the global distribution of the Quasi-Biennial Oscillation in the OSU2 GCM. A comparison between the OSU2 GCM and OSU6 GCM in terms of all the signals seen in Figure 1 is presented in a forthcoming paper [Hameed and Currie, 1990].

An approach to understanding the physical meaning of the spectrum in Figure 1c is suggested by recalling that combination tones are generated in nonlinear systems. Let us take, following Feynman et al. (1963), the output response $x_{out}(t)$ to be related to the input $x_{in}(t)$ in a nonlinear system (with ϵ small compared to unity) by

$$x_{out} = K(x_{in} + \epsilon x_{in}^2) \qquad (1)$$

where K is constant. Letting the input function be $x_{in} = A\cos\omega_1 t + B\cos\omega_2 t$, where ω_1 and ω_2 are not in a harmonic relation, there will be a component in x_{out} given by

$$x_{out} = AB\cos\omega_1 t\cos\omega_2 t = AB/2[\cos(\omega_1 + \omega_2)t + \cos(\omega_1 - \omega_2)t].$$

We thus see that two new components have been produced, one at the sum frequency $(\omega_1 + \omega_2)$, and another at the difference frequency $(\omega_1 - \omega_2)$, where ω_1 and ω_2 may be called "parent" frequencies of the combination tones $(\omega_1 \pm \omega_2)$.

Referring again to Figure 1 we may consider the sub-annual frequencies at $T_1 \simeq 40$ months, $T_2 \simeq 26.7$ months, and $T_3 \simeq 14.4$ months, and the annual period and its harmonics as "parents". The combination tones are then given by

$$f_{i\pm j} = 1/T_i \pm (j+1)/12 \text{ cycles per month} \qquad (2)$$

with

$$i = 1,2,3, \text{ and } j = 0,\ldots,5.$$

The three tones f_{i+5} cannot be detected in data sampled monthly because they lead to periods shorter than 2 months. Therefore, theoretically we have 11 tones for each sub-annual signal or 33 tones altogether as tabulated in Table 1.

Table 1. Summary of theoretical and observed summation and difference tones in terms of frequencies and periods. See Figure 1c for observations.

Tones	$f_{i\pm j}$ eqn. 1	Predicted frequency (cpm)	Observed frequency (cpm)	% out of 216 spectra	Discrepancies	Predicted period (months)	Observed period (months)
1	f_{3-0}	0.01407	0.01453	97	-0.00046	71.06	68.82
2	f_{2-0}	0.04583	0.04990	56	-0.00407	21.82	20.04
3	f_{1-0}	0.05835	0.05844	42	-0.00009	17.14	17.11
4	f_{3-1}	0.09741	0.09746	93	-0.00005	10.27	10.26
5	f_{1+0}	0.10831	0.10823	61	0.00008	9.23	9.24
6	f_{2+0}	0.12083	0.11658	57	0.00425	8.28	8.58
7	f_{2-1}	0.12917	0.12504	36	0.00413	7.74	8.00
8	f_{1-1}	0.14169	0.14176	66	-0.00007	7.06	7.05
9	f_{3+0}	0.15259	0.14989	94	0.00270	6.55	6.67
10	f_{3-2}	0.18074	0.18383	77	-0.00309	5.53	5.44
11	f_{1+1}	0.19165				5.22	
12	f_{2+1}	0.20417	0.20028	31	0.00389	4.90	4.99
13	f_{2-2}	0.21250	0.21677	89	-0.00427	4.71	4.61
14	f_{1-2}	0.22502	0.23133	80	-0.00631	4.44	4.32
15	f_{3+1}	0.23593	0.24171	36	-0.00578	4.24	4.14
16	f_{3-3}	0.26407	0.26432	78	-0.00025	3.79	3.78
17	f_{1+2}	0.27498	0.27303	63	0.00195	3.64	3.66
18	f_{2+2}	0.28750				3.48	
19	f_{2-3}	0.29583	0.29416	86	0.00167	3.38	3.40
20	f_{1-3}	0.30835	0.30828	34	0.00007	3.24	3.24
21	f_{3+2}	0.31926	0.320[illegible]6	34	-0.00140	3.13	3.12
22	f_{3-4}	0.34741	0.35009	37	-0.00268	2.88	2.86
23	f_{1+3}	0.35831	0.36048	100	-0.00217	2.79	2.77
24	f_{2+3}	0.37083	0.37289	77	-0.00206	2.70	2.68
25	f_{2-4}	0.37917	0.38316	38	-0.00399	2.64	2.61
26	f_{1-4}	0.39163				2.55	
27	f_{3+3}	0.40259	0.39931	98	0.00328	2.48	2.50
28	f_{3-5}	0.43074	0.43151	74	-0.00077	2.32	2.32
29	f_{1+4}	0.44165	0.44400	79	-0.00235	2.26	2.25
30	f_{2+4}	0.45417	0.45537	78	-0.00120	2.20	2.20
31	f_{2-5}	0.46250				2.16	
32	f_{1-5}	0.47502	0.47518	41	-0.00016	2.11	2.10
33	f_{3+4}	0.48593	0.48321	27	0.00272	2.06	2.07
			Mean		-0.00057		
			Standard Deviation		±0.00283		

Table 1 also presents the comparison of theory with observation in terms of frequencies and periods. We see that 29 of the tones found in the Oregon State GCM, shown in Figure 1c, correspond to the predictions of eqn. (2). The exceptions are the two peaks with periods 2.03 and 2.93 months in Figure 1c. In Table 1 we note that four frequencies (tones 11, 18, 26, and 31) predicted by eqn. (2) are not produced in the GCM at these latitudes. In column 5 we give the percentage of the spectra in which a given peak is found. At ten frequencies (tones 3, 7, 12, 15, 20-22, 25, 32-33) the observed peaks are found in less than half of the 216 spectra; for the remaining 19 tones the mean percentage is 79%. Column 6 of Table 1 gives the discrepancies of observation from theory with respect to frequencies, and for the 29 tones the mean discrepancy is -0.00057 ± 0.00283 cycles per month as shown.

Table 2 shows the contribution in percent of total variance for the various signals and noise at high northern latitudes. The summed variance contribution for all the signals in Figure 1 for latitudes 74-82° was 51.1%, while 49.9% was con-

Table 2. Percentages of variance contained in three classes of signals and noise in three latitude zones.

Latitutes	Sub-annual signals T_1, T_2, T_3	Annual + harmonics	Combination tones	Sum of all signals	Noise
86-90	5.4%	11.4%	35.1%	51.9%	48.1%
74-82	4.4	27.6	19.1	51.1	49.9
58-70	1.7	58.0	5.0	64.7	35.3

tained in the background noise. The combination tones contribute 19% of the variance in this latitude range and 35% in the polar regions. Thus, a substantial fraction of high-latitude climatic variability is explained by the output response tones, which are generated by interaction between the input sub-annual signals and the annual term and its harmonics. In Table 2 we note that the relative contributions of the combination tones decrease with decreasing latitude, while those of the annual cycle and its harmonics increase. Over most of the earth the annual term and harmonics contribute to well over half of total variance.

Discussion

On initial inspection the many spectral lines in Figure 1c appear to be confusing. The writers were led to the physical explanation presented in Table 1 in an incremental manner. For example, when Hameed and Currie (1989) submitted their original manuscript for review they stated that no explanation could be provided for the term near 10 months. It was only after the manuscript was accepted for publication that we realized the ca. 10 month period is the difference frequency f_{3-1} between the Chandler and 6 month harmonic. This, in turn, led to the results presented here.

Since the spectrum of atmospheric pressure is not continuous, but consists of discrete and physically explained lines, the climate system may not be characterized as chaotic on these time scales. Attempts to describe atmospheric variations as a chaos process [see Pool, 1989] originated from simulations of atmospheric circulation in highly simplified models [Lorenz, 1963]. In these simulations the temporal variation of solar radiation was neglected, and thus the physical phenomena listed in columns 2-4 of Table 2 could not be produced; only the noise listed in column 6 was simulated and identified as the dominant characteristic of weather and climate.

The analysis of climate simulated in the more realistic General Circulation Model presented here suggests that inclusion of the correct temporal and spatial variation of solar radiation input into the atmosphere-ocean system is essential to a physically proper description of the system. The periodic solar variations impose order on the system as described in this paper. Prigogine (1947) has shown that energy input into a system results in steady non-equilibrium states characterized by a minimum of entropy production, i.e., by order, and Wyant et al. (1987) have demonstrated that Prigogine's theorem is applicable to the climate system only if time dependence of solar radiation is included in model calculations.

Acknowledgments. We thank Dr. G. L. Potter and Dr. W. L. Gates of Lawrence Livermore Laboratory for sending the GCM time series to us for analysis. This work was performed under the auspices of the CO_2 Research Division, Office of Basic Energy Sciences, U. S. Department of Energy through Grant DEFG0285ER60314A007 to the State University of New York at Stony Brook.

References

Currie, R. G. and S. Hameed, Evidence of quasi-biennial oscillations in a general circulation model, Geophys. Res. Lett., 15, 649-652, 1988.

Feynman, R. P., R. B. Leighton, and M. Sands, The Feynman Lectures on Physics, Vol. 1, Addison-Wesley, Reading, 1963.

Gates, W. L., Y. Han and M. Schlesinger, The global climate simulated by a coupled atmosphere-ocean general circulation model: Preliminary results, Coupled Ocean-Atmosphere Models, Ed. J. Nihoul, Elsevier, 131-152, 1985.

Hameed, S. and R. G. Currie, Simulation of the 14-month Chandler wobble in a global climate model, Geophys. Res. Lett., 16, 247-250, 1989.

Hameed, S., K. R. Sperber and R. D. Cess, Genesis of the Southern Oscillation within the atmosphere: illustration with general circulation models, Geophys. Res. Lett., 16, 691-694, 1989.

Hameed, S., R. G. Currie, and H. Lagrone, Atmospheric oscillations from 2 to 70 months in a general circulation model, in preparation, 1990.

Hameed, S. and R. G. Currie,, Comparison of signals in two coupled ocean-atmosphere general circulation models, To be presented at Beijing International Symposium on Climatic Change, August 1990.

Lorenz, E. N., Deterministic nonperiodic flow, J. Atmos. Sci., 20, 130-141, 1963.

Pool, R., Is something strange about the weather?, Science, 243, 1290-1293, 1989.

Prigogine, I., Etude Thermodynaminque Des Phenomenes Irreversibles, Chapter V, Desver, Liege, 1947.

Sperber, K. R., S. Hameed, W. L. Gates and G. L. Potter, Southern oscillation simulated in a global climate model, Nature, 329, 140-142, 1987.

Sperber, K. R., Southern Oscillation Simulation in Coupled Ocean/ Atmosphere Global Climate Models, Ph.D. Thesis, State University of New York at Stony Brook, 1989.

Stoker, J. J., Nonlinear Vibrations in Mechanical and Electrical Systems, Interscience, New York, 1950.

Wyant, P. H., A. Mongroo and S. Hameed, Determination of Heat Transport Coefficient in Energy-Balance Climate Models of Extremization of Entropy Production, J. Atmos. Sciences, 45, 189-193, 1988.

Robert G. Currie and Sultan Hameed, Institute for Terrestrial and Planetary Atmospheres, State University of New York, Stony Brook, NY 11794

(Received July 13, 1989;
revised April 16, 1990;
accepted April 23, 1990)